TOPICAL REVIEW — Magnetism, magnetic materials, and interdisciplinary research

Nanomagnetism: Principles, nanostructures, and biomedical applications*

Yang Ce(杨 策)[a], Hou Yang-Long(侯仰龙)[a]†, and Gao Song(高 松)[b]

[a] Department of Materials Science and Engineering, College of Engineering, Peking University, Beijing 100871, China
[b] College of Chemistry and Molecular Engineering, Peking University, Beijing 100871, China

(Received 27 March 2014; published online 15 April 2014)

Nanomagnetism is the origin of many unique properties in magnetic nanomaterials that can be used as building blocks in information technology, spintronics, and biomedicine. Progresses in nanomagnetic principles, distinct magnetic nanostructures, and the biomedical applications of nanomagnetism are summarized.

Keywords: nanomagnetism, magnetic materials, magnetic resonance imaging (MRI), magnetic hyperthermia

PACS: 75.75.–c, 81.07.–b, 75.50.–y, 87.80.Lg **DOI:** 10.1088/1674-1056/23/5/057505

1. Introduction

The study of nanomagnetism aims to deal with the magnetic properties of materials that have at least one dimension in the size range from 1 nm to 100 nm. A nanomagnetic material exhibits magnetic behaviors that are distinct from those of the bulk form of the same substance[1,2] because (i) the material's dimensions are comparable to the critical lengths of one or more of various physical phenomena, such as the size of the magnetic domains;[3–5] (ii) the translation symmetry is broken, giving rise to specific sites with reduced coordination numbers, broken exchange bonds, and frustration;[6,7] (iii) the material is in close contact with an exterior system such as the substrate or capping layer in the thin film magnets;[8,9] (iv) the spin wave spectrum is changed because the spin wave energy is comparable to the thermal energy.[10] As a result of their extraordinary magnetic behaviors, nanomagnets have many practical applications distinct from those of the conventional bulk magnets, such as magnetic recording, giant magnetoresistance (GMR) devices, magnetic resonance imaging (MRI), magnetic hyperthermia and bionsensors.[11–18]

In this article, we will introduce several important nanomagnetic effects, and then discuss the magnetism properties of diverse magnetic nanostructures. Finally, the applications of nanomagnetism in biomedicine are also addressed.

2. Nanomagnetic effects

2.1. Single domain and superparamagnetism

The subdivision of a material into distinct magnetic domains is the origin of many unique behaviors of magnetic materials. For example, differing magnetic directions of domains may give rise to the dissolution of the total magnetic moment, or an average magnetization approximating zero. Based on the theory of magnetism, taking an ellipsoid for example, the total energy is contributed by three types of energies, exchange, anisotropy, and magnetostatic energy. With the increase in the size of a magnet, the number of domains will also increase. As a result, there will be a decrease in the magnetostatic energy, while the more numerous domain walls will also raise the exchange and the anisotropy energies. Therefore, the size of the magnet has a great influence on its magnetic behavior, as can be illustrated by considering the coercivity of the magnet.[19] The size-dependent coercivity of magnets is shown schematically in Fig. 1.[20–22] First, for very small particles whose diameters are smaller than the critical diameter of superparamagnetism ($D_{\rm spm}$), the magnetic moment is not stable, and therefore $H_{\rm c} = 0$. Secondly, in the range between $D_{\rm spm}$ and the critical diameter of a single domain ($D_{\rm sd}$), the moment is stable, and the coercivity enlarges as $D_{\rm sd}$ increases. Finally, for larger diameters, the multi-domain region appears, and the coercivity declines with increasing particle diameter. Therefore, the magnet has the maximal coercivity when its diameter is equal to $D_{\rm sd}$, and it will become superparamagnetic when its diameter becomes smaller than $D_{\rm spm}$.

In particular, for the single domain magnet, all the magnetic moments are along the anisotropy axis, and the free energy contribution from exchange and anisotropy is zero. Therefore, the magnetostatic energy is the only relevant energy term. Moreover, as shown in Fig. 2, the $D_{\rm sd}$ of magnetic materials has a close relationship with the anisotropy constant K, and for the identical saturation magnetization ($M_{\rm s}$), $D_{\rm sd}$ is

*Project supported by the National Basic Research Program of China (Grant No. 2010CB934601), the National Natural Science Foundation of China (Grant Nos. 51125001 and 51172005), the Natural Science Foundation of Beijing, China (Grant No. 2122022), and the Doctoral Program, China (Grant No. 20120001110078).

†Corresponding author. E-mail: hou@pku.edu.cn

© 2014 Chinese Physical Society and IOP Publishing Ltd

also proportional to the domain wall energy. In addition to that, with the increase of the domain wall energy, the critical single domain diameter D_{sd} will also increase.[23]

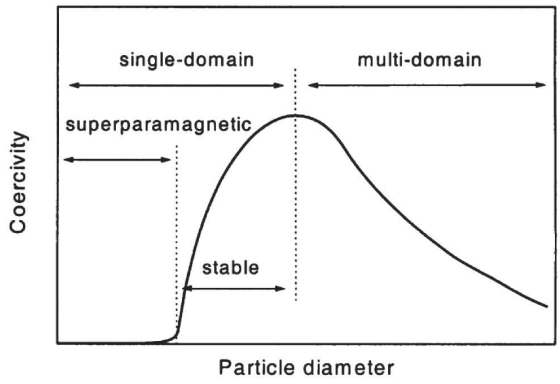


Fig. 1. Size dependence of coercivity of magnets.

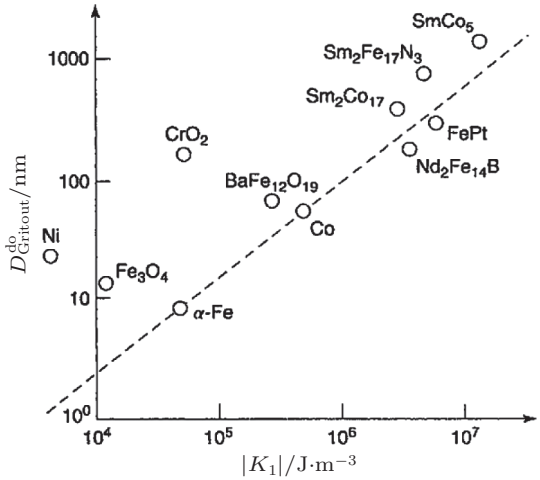


Fig. 2. Relationship between D_{sd} and the anisotropy constant for magnetic materials.[23]

When the size of the particles is sufficiently small, the thermal energy will be able to overcome the anisotropy energy. Thus, the magnetization is no longer in a stable configuration. The temperature at which the thermal energy can overcome the anisotropy barrier of nanoparticles (NPs) is referred to as the blocking temperature (T_B).[24] The critical diameter D_{spm} is the maximum size below which, at given temperature, the superparamagnetism behavior takes place.[6,25]

2.2. Exchange-coupling effect

Since the first model of the exchange-coupling effect was introduced by Kneller and co-workers, this effect attracts intense interest. The exchange-coupling effect only takes place at the interphase boundary between hard and soft magnets at nanoscale,[26] and an exchange-coupled magnet can be designed based on the expected properties by choosing various hard and soft phases and tuning the phase ratio.[27] In an exchange-coupled magnet, nanoscale hard and soft magnetic phases are coupled via the interfacial exchange interaction such that the soft phase becomes "hardened" and its high magnetization enhances the energy product $(BH)_{max}$ of the composite (Fig. 3).[28] The energy arising from the exchange-coupling effect is given by

$$E = -J \cdot \mu_1 \cdot u_2 \cos\theta,$$

where μ_1 and μ_2 are the magnetic moments of the two phases and $\cos\theta$ denotes the angle between them. Moreover, J represents the exchange-coupling constant, which describes the intensity of the magnetic coupling and is closely related to the arrangements of the magnetic moments.

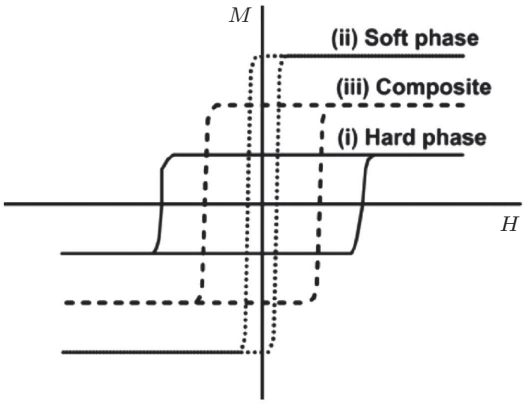


Fig. 3. Typical hysteresis loops: (i) a hard phase, (ii) a soft phase, (iii) the exchange-coupled nanocomposites made of the soft and hard phases.[28]

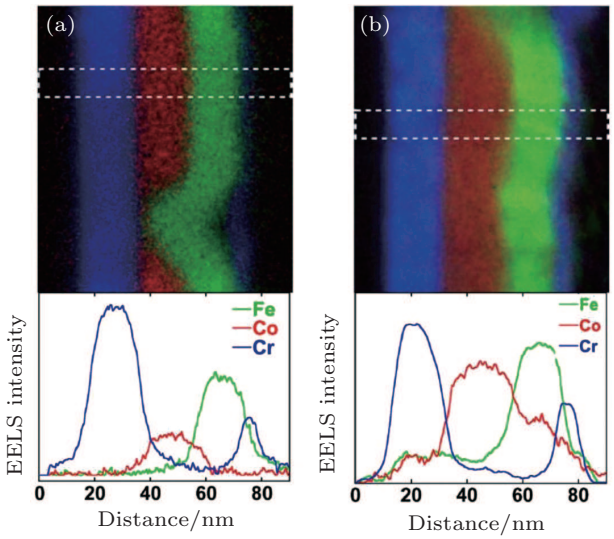


Fig. 4. EELS elemental maps and line scans of Sm–Co (20 nm)/Fe(20 nm) samples with (a) sputtering temperature at 100 °C and (b) annealing temperature at 400 °C.[30]

Recently, the importance of the interphase layer to the exchange-coupling effect is frequently suggested. It is generally accepted that the energy generated from exchange coupling does not depend sensitively on the exchange constant J, but instead depends on the exchange constant and the thick-

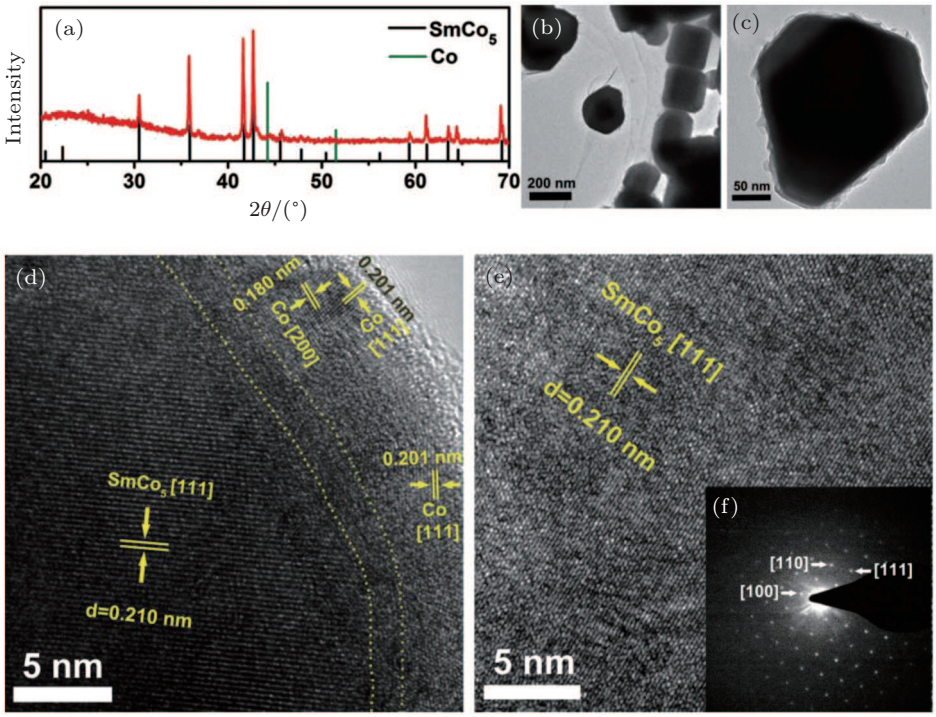


Fig. 5. (a) XRD pattern of $SmCo_5$@Co nanomagnets. (b) and (c) TEM images of as-synthesized SmCo5@Co magnets. (d) and (e) HRTEM images of (d) the exterior of and (e) an arbitrary interior part of the particle. (f) SAED pattern of the particle shown in panel (c).[31]

ness of the soft phase.[29] In the case of Sm–Co based nanocomposites, Liu and coworkers developed graded interfacial layers in which the material parameters gradually varied by promoting the intermixing of Sm–Co with Fe via thermal treatments at elevated annealing temperatures (Fig. 4).[30] Hou and coworkers found that an amorphous intermediate layer appeared in chemically synthesized $SmCo_5$@Co core-shell nanomagnets (Fig. 5).[31] It was found that the magnetization behavior of the modified interface differs notably from that of a sharp interface and relaxes the grain size requirement for optimal exchange–spring properties.[30–32] However, in the case of a series of L_{10}-FePt based exchange-coupling nanomagnets, Hou and coworkers found that no significant alloying took place at the interface, and a single phase behavior was also displayed with the absence of an interphase layer.[33]

In the Nd–Fe–B-based exchange-coupled magnets, however, the interphase gradient does not enhance the ferromagnetic properties, but rather leads to severe deterioration. The introduced magnetic soft phase likely alloys with the hard phase. Unlike $SmCo_5$ based nanocomposites, there are no pinning sites in the Nd–Fe–B phase, and therefore, the coercivity of the exchange-coupled Nd–Fe–B/Fe composite is much lower than that of the Nd–Fe–B magnets.[34,35] Thus, to avoid this phenomenon, a sharp interphase boundary, with no alloying, is required. By using a Ta layer as an interfacial layer, Hono and coworkers prepared $Nd_2Fe_{14}B$/FeCo thin film magnets with an enhanced maximum energy product $(BH)_{max}$ (Fig. 6).[36]

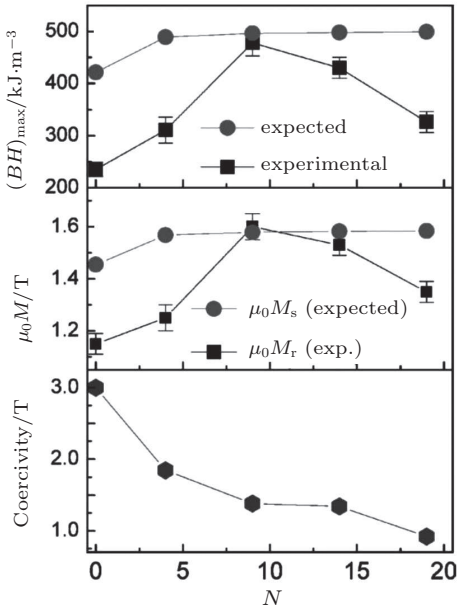


Fig. 6. (a) Coercivity, (b) remanence, and (c) $(BH)_{max}$ dependencies on the number of layers N in multilayer films of Ta(50 nm)[Nd–Fe–B(30 nm)/Nd(3 nm)/Ta(1 nm)/Fe67Co33 (10 nm)/Ta(1 nm)]$_N$/Nd–Fe–B(30 nm)/Nd(3 nm)/Ta(20 nm).[36]

2.3. Exchange bias effect

The exchange bias effect originates in the interaction through the interface between any two of ferromagnetic (FM), antiferromagnetic (AFM), and ferromagnetic (FI) domains. Generally, this interaction acts as an effective field that changes the behavior of the ferromagnet under an applied magnetic field, which is manifest as a displacement of the hysteresis loop.[19]

The effect was first discovered in the studies of field-cooled (FC) oxidized Co particles, in which the relevant interface was that between the Co grains (FM) and the surrounding CoO layer (AFM).[37]

The hysteresis loop of exchange bias magnets is shown schematically in Fig. 7.[38] Starting from magnetic saturation (a), as the field reverses, the FM moments begin to flip (b), but the AFM atoms exert a local restoring force due to the magnetic field from the interface. Since the AFM atoms exhibit a torque dragging the FM moments to their initial direction, this effect is called unidirectional anisotropy. Note that the resulting displacement of the hysteresis curve is proportional to the effectiveness of the coupling between the two layers.[19]

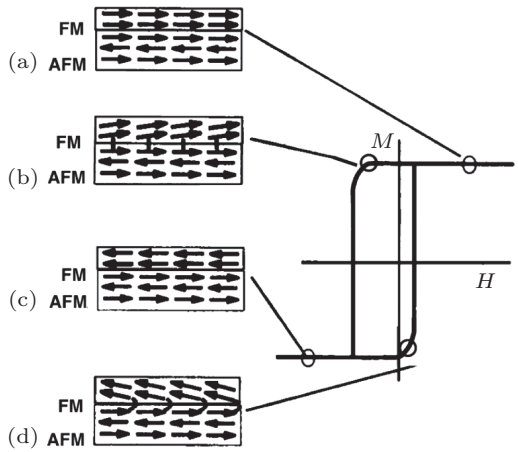


Fig. 7. Schematic diagram of the spin configurations of an FM–AFM bilayer.[38]

Moreover, due to the requirement to overcome the AFM anisotropy during the magnetization reversal in the FM phase, the coercivity of the composite magnet increases. This well known coercivity-increase effect is another important characteristic of exchange bias magnets. Recently, Hadjipanayis and coworkers prepared 4 nm ferromagnetic cobalt nanoparticles (NPs) embedded in either a paramagnetic or an antiferromagnetic matrix, and it was found that the cobalt cores lost their magnetic moment at 10 K in the first system, while remaining ferromagnetic up to about 290 K in the second one (Fig. 8). It was demonstrated that the phenomenon can be ascribed to the specific way that the ferromagnetic NPs couple to the antiferromagnetic matrix.[39]

Another phenomenon that shows up in systems with exchange bias is the training effect, i.e., the exchange bias field is found to depend on the number of measurements performed, decreasing as this number increases.[40] Zhang and coworkers observed the exchange bias and the training effect in γ-Fe_2O_3-coated Fe NPs. It was found that the field-cooling hysteresis shifts in both the horizontal and the vertical directions due to the change in spin configuration arising from field cycling during the hysteresis loop measurements (Fig. 9). The decrease of the frozen spins along the cooling field direction reduces the effective pinning energy, and thus, the exchange bias field decreases with field cycling.[41]

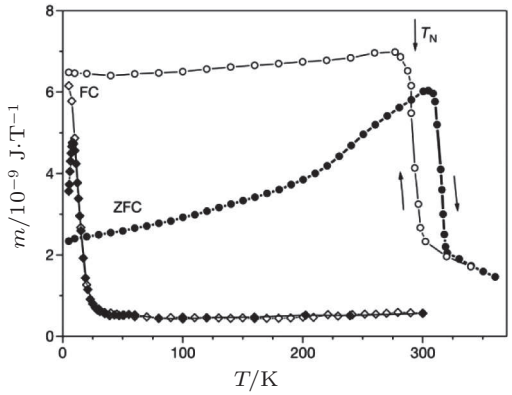


Fig. 8. Temperature dependences of the zero-field cooled (ZFC; filled symbols) and the field-cooled (FC; $\mu_0 H_{FC} = 0.01$ T, open symbols) magnetic moments of 4-nm Co/CoO core-shell particles. Particles were embedded in a paramagnetic (Al_2O_3) matrix (diamonds), or in an AFM (CoO) matrix (circles).[39]

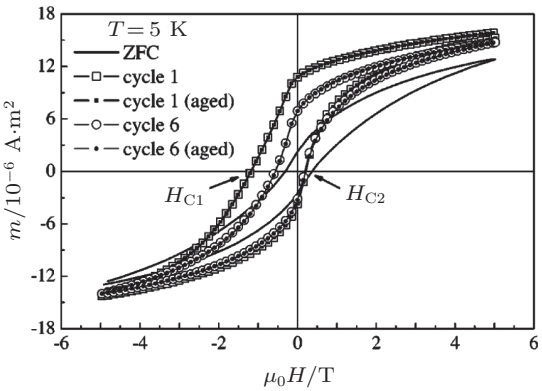


Fig. 9. The ZFC loop, first and sixth FC loops, and aged first and sixth FC loops at 5 K.[41]

During a field-cooling process, when the temperature is above the Neel temperature (T_N) of the antiferromagnet and below Curie temperature (T_C) of the ferromagnet, the magnetic moments of the AFM atoms are disordered. However, as T_N is reached, the AFM atoms at the interface align ferromagnetically to the FM moments.

3. Magnetism of nanomaterials

3.1. Magnetism of NPs

The Stoner–Wolfforth model was the first model to describe the magnetism of small particles and is still used today.[42] In this model, each NP is considered as a homogeneous single domain with an elongated ellipsoid shape. However, the model does not take into account the possibility of thermal excitation to overcome the energy barrier between the two magnetization directions, which means that this model is only suitable at $T = 0$ K.[19] Moreover, the model is applicable only to NPs with uniaxial anisotropy. For cubic anisotropy,

however, a three-dimensional model is required to describe the magnetism.

In addition to the single domain magnetism and superparamagnetism mentioned in Section 2.1, another important feature of any NP is its large surface to volume ratio. It has been proposed that the large surface to volume ratio enhances the magnetic moment and the anisotropy. And enhancements in magnetic moments have in fact been observed for Fe, Co, and Ni NPs with several tens to several hundreds of atoms.[7,10,43–45]

3.2. Magnetism of nanoplates

Circular magnetic nanostructures, such as nanoplates, are promising materials in the development of higher performance magnetic information storage devices.[46–48] In nanoplates with thickness of several nanometers, the magnetization is almost entirely restricted to the plane of the plate. However, close to the center of the plate, there is a vortex.

The equilibrium arrangement for the magnetic moment of the nanoplate is such that the magnetic moment orientation points outward at the center of the plane, which means that a perpendicular component of the magnetization exists at the center of the plate.[49] This vortex core has been detected by magnetic force microscopy (MFM). MFM images show dark or light dots at the centers of the disks, representing upward or downward vortex core magnetization. The Z component of the magnetization of the vortex core can point up and down during the rotation of the vortex in clockwise (CW) or counterclockwise (CCW) directions. As a result, the chirality of the vortex can be identified by the combination of vortex core polarity and rotation of the vortex.[50] When an in-plane magnetic field is applied, the chirality can be found from the motion of the vortex core. The motion is generated by the torque on the magnetic moment in the vortex.[51] This unique property has great application potential in the area of recording media.

3.3. Magnetism of nanorings

Generally, the magnetism of nanorings is quite similar to that of nanoplates. However, compared with nanoplates, nanorings show superior potential in magnetic recording applications due to the allowance for higher storage density generated from their flux-closed structure and stable magnetic reversal behavior.[52] Three kinds of magnetizations have been observed in nanorings: (A) the moment follows the same rotation direction and forms a vortex; (B) the nanoring is partitioned into two magnetic domains, in which the two moments are opposite in direction (this also called an onion state); (C) the twisted state, or asymmetric onion state, frequently found in nanorings of smaller size.[19] An applied magnetic field in the onion state can move the domain walls to coalesce on the opposite side of the ring, and therefore, forming a new configuration at remanence.[52–54]

Sun and co-workers looked into the magnetic properties of Fe_3O_4 nanorings. They suggested that there are two kinks in the hysteresis loop near zero-magnetization, revealing that there are two vortex states with opposite directions (insets of Fig. 10(a)). The HRTEM image (Fig. 10(b)) shows that the Fe_3O_4 nanorings have two directions, $\langle 111 \rangle$ and $\langle 112 \rangle$ with magnetic vortex states (Fig. 10(c)).[55]

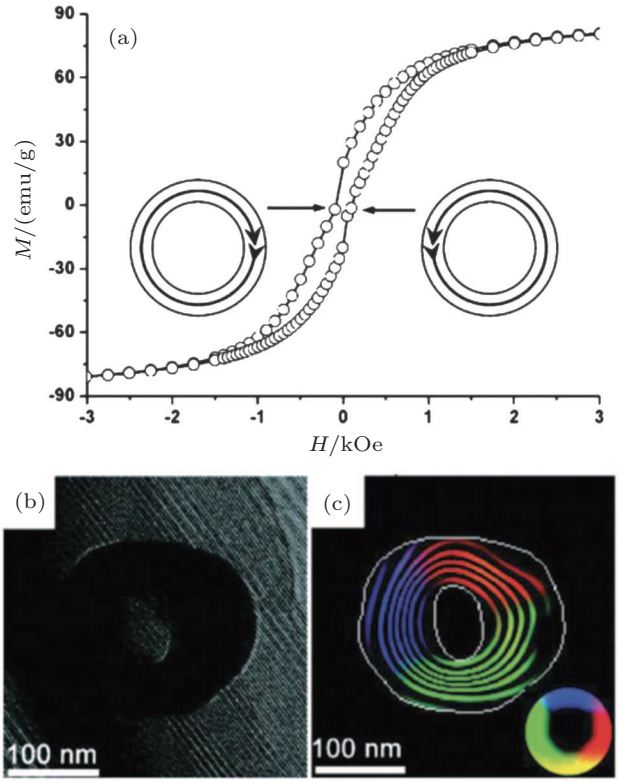


Fig. 10. (a) The M–H loop of the Fe_3O_4 mnanorings under room temperature. (b) Off-axis electron hologram of a single Fe_3O_4 ring. (c) Direction of the magnetic induction under field-free conditions following magnetization, indicated by colors as interpreted in the color wheel in the inset (red = right, yellow = down, green = left, blue = up).[55]

4. Biomedical applications of nanomagnetism

4.1. $T2$ MRI contrast agents

Magnetic resonance imaging is a fundamental diagnostic tool in biomedical fields. MRI contrast agents can help to clarify images, allowing better interpretation. Theoretically, when the nuclei of protons are exposed to a strong magnetic field, their spins are arranged along the magnetic field. During the alignment, the spins process with a particular frequency, called the Larmor frequency (Fig. 11(a)). When a pulse with the resonance frequency in the radio-frequency (RF) range is introduced, the protons are excited to the antiparallel state. Then, after the removal of the pulse, the excited nuclei will relax to the initial states through either the $T1$ relaxation pathway, which involves the decreased net magnetization (M_z), recovering to the initial state, or the $T2$ relaxation, which involves the induced magnetization on the perpendicular plane (M_{xy})

disappearing by the dephasing of the spins (Figs. 11(c) and 11(d)).[56]

When the magnetic pulse is applied, a transverse magnetization perpendicular to the static magnetic field is generated (Fig. 11(b)). And thus, the magnetization is composed of M_z and M_{xy}, which produce the interrelated process of spins. The energy transfer is responsible for the change of M_z, while the reason for the change of M_{xy} is spin dephasing, which is the randomization of the magnetization of the excited spins that were originally of the same phase coherence immediately after the application of the pulse, but the coherence disappeared because of the difference of the magnetic field experienced by the protons.[56–58] The phase incoherence is largely caused by the magnetic properties of the imaging objects, while the magnetic-field difference arises mainly from other different magnetic properties of the imaging objects. The spin–spin interaction between the protons or electrons causes a loss of transverse coherence, which produces the true and characteristic $T2$ relaxation of tissues. Moreover, this interaction will also induce local magnetic field gradients, which can also be generated by contrast agents. Thus, the transverse relaxation is affected by external sources, and the total relaxation time $T2^*$ is described by $1/T2^* = (1/T2) + \gamma B$, where γB represents the relaxation by the field gradients and is called the susceptibility effect.[56] The $T2$ relaxivity is highly dependent on both the M_s value and the effective radius of the typically superparamagnetic core. In the motional average regime, the relaxivity r_2 (where all of the NP contrast agents are simulated as spheres) is given by

$$r_2 = \left(\frac{256\gamma^2\pi^2}{405}\right)\kappa M_s^2 r^2/D(1+L/r),$$

where M_s and r are the saturation magnetization and the effective radius of the magnetic nanostructure, respectively, D is the diffusivity of water molecules, L is the thickness of an impermeable surface coating, and k is the conversion factor.[59]

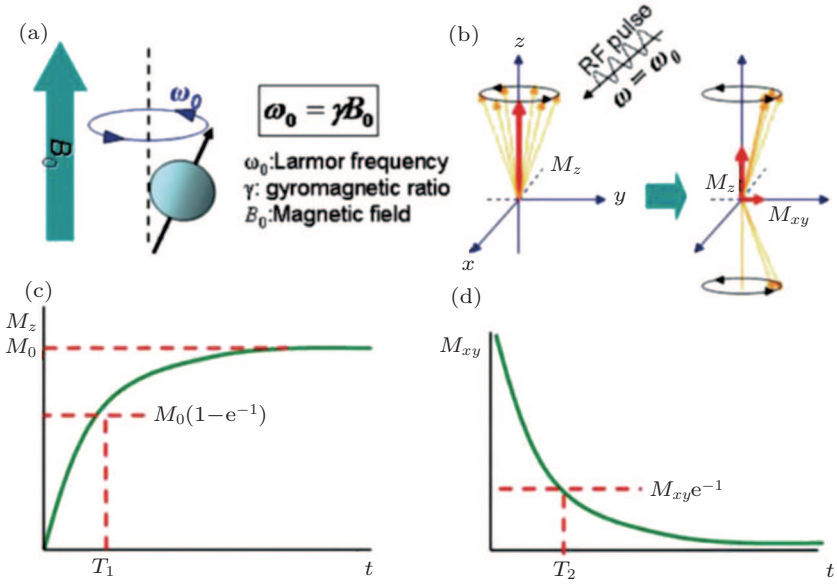


Fig. 11. Schematic illustration of magnetic resonance imaging. (a) Spins align parallel or antiparallel according to the magnetic field and process under Larmor frequency ω_0. (b) After induction of the pulse, magnetization of spins changes. Excited spins are relaxed through (c) $T1$ relaxation or (d) $T2$ relaxation.[56]

4.2. Magnetic hyperthermia

Magnetic NPs with spherical magnetic moments undergo orientational thermal fluctuations due to either Brownian fluctuations or Neel fluctuations. These fluctuations are the reasons for the magnetization relaxation that takes place in a suspension of superparamagnetic particles when the magnetic field is removed. An external AC magnetic field supplies energy that generates the magnetic moment fluctuations, and this magnetic energy is converted into thermal energy.[60,61]

The heating effects of magnetic NPs under AC magnetic fields are related to several types of loss processes (hysteresis losses, Neel and Brown relaxations), and which of these processes contribute strongly depends on the particle size. For NPs within the single-domain range, the magnetization relaxation is governed by the combined effects of the rotational external (Brownian) and internal (Neel) diffusions of the particles' magnetic moments. The Brown relaxation is due to thermal orientational fluctuations of a grain itself in the carrier fluid, the magnetic moment being locked onto the crystal anisotropy axis. The Neel relaxation refers to the internal thermal rotation of the magnetic moment of the particle within the crystal.[60]

The specific heat dissipation for monodisperse magnetic NPs is expressed as

$$\mathrm{SLP} = \frac{P}{\rho\phi} = \frac{\mu_0\chi_0 H_0^2}{2\rho\phi}\omega\frac{\omega\tau}{1+(\omega\tau)^2},$$

where χ_0 is the static susceptibility, μ_0 is the vacuum magnetic permeability, ρ is the density of the material, H_0 is the applied field, and ω is the frequency of the applied field. Moreover, τ is given by the relationship $1/\tau = 1/\tau_{\mathrm{N}} + 1/\tau_{\mathrm{B}}$, where τ_{N} is the Neel relaxation time and τ_{B} is the Brownian relaxation time, as will be described below.[60,61]

4.3. Biosensors

In addition to their applications in disease dignoses and therapy, magnetic NPs have been utilized in various biosensors such as those for the detection of proteins, DNAs, and enzymes. Due to the unique chemical and physical properties of magnetic NPs, incorporating them in biosensors can improve the sensors' sensitivity and reduce their reaction time. In the case of magnetic NP-based MRI $T2$ contrast agents, researchers observed a special magnetic phenomenon in the process of the assembly of magneitc nanoprobes under a magnetic field, i.e., the superparamagnetic iron oxide cores of individual NPs were more efficient in dephasing the spins of surrounding water protons, and thus expanding the spin–spin relaxation time. Magnetic NPs were proposed as magnetic relaxation switches (MRS).[62] Therefore, by surface modification, a large number of magnetic NPs can be selectively attached to nuclei acids, peptides, proteins, and antibodies. As a result, the change of the relaxation time of protons will be produced by those aggregated NPs and cause the detection of special oligonucleotides, as mentioned above. This method can be further extended in the detection of molecular interactions such as DNA–DNA and protein–protein.[63]

5. Conclusion

We have presented typical magnetic effects that commonly appear in nanomagnetic materials. Those effects are the origins of many unique properties of nanosized magnetic materials. Significant progress is being made in exploring the fundamentals of magnetism as well as in developing magnetic materials. And this stimulate great expectations for the use of those theories and materials in new devices with enhanced performance. Nowadays, magnetic nanostructures have already been important in biomedical applications such as MRI, hyperthermia, and biosensors. And other physical effects of nanomagnets, including distinct vortex states, exchange coupling, and exchange bias effects have great application potential in energy conversion, household electrical equipments, and electronic devices.

References

[1] Sellmyer D J, Zheng M and Skomski R 2001 *J. Phys.: Condens. Matter* **13** R433
[2] Wu C Z, Yin P, Zhu X, OuYang C Z and Xie Y 2006 *J. Phys. Chem. B* **110** 17806
[3] Kim D, Lee N, Park M, Kim B H, An K and Hyeon T 2009 *J. Am. Chem. Soc.* **131** 454
[4] Kovalenko M V, Bodnarchuk M I, Lechner R T, Hesser G, Schaffler F and Heiss W 2007 *J. Am. Chem. Soc.* **129** 6352
[5] Zhang L H, Wu J J, Liao H B, Hou Y L and Gao S 2009 *Chem. Commun.* **454** 378
[6] Knobel M, Nunes W C, Socolovsky L M, De Biasi E, Vargas J M and Denardin J C 2008 *J. Nanosci. Nanotechno.* **8** 2836
[7] Billas I M L, Chatelain A and Deheer W A 1994 *Science* **265** 1682
[8] Chen J, Ye X C, Oh S J, Kikkawa J M, Kagan C R and Murray C B 2013 *ACS Nano* **7** 1478
[9] Fedoseev S A, Pan A V, Rubanov S, Golovchanskiy I A and Shcherbakova O V 2013 *ACS Nano* **7** 286
[10] Shen J and Kirschner J 2002 *Surf. Sci.* **500** 300
[11] Yang C, Zhao H B, Hou Y L and Ma D 2012 *J. Am. Chem. Soc.* **134** 15814
[12] Liu F, Jin Y J, Liao H B, Cai L, Tong M P and Hou Y L 2013 *J. Mater. Chem. A* **1** 805
[13] Jin Y J, Liu F, Tong M P and Hou Y L 2012 *J. Hazard Mater.* **227** 461
[14] Takatsu H, Ishikawa J J, Yonezawa S, Yoshino H, Shishidou T, Oguchi T, Murata K and Maeno Y 2013 *Phys. Rev. Lett.* **111**
[15] Yang D Z, Wang F C, Ren Y, Zuo Y L, Peng Y, Zhou S M and Xue D S 2013 *Adv. Funct. Mater.* **23** 2918
[16] Hayashi K, Ono K, Suzuki H, Sawada M, Moriya M, Sakamoto W and Yogo T 2010 *Chem. Mater.* **22** 3768
[17] Das M, Dhak P, Gupta S, Mishra D, Maiti T K, Basak A and Pramanik P 2010 *Nanotechnology* **21** 125103
[18] Polito L, Colombo M, Monti D, Melato S, Caneva E and Prosperi D 2008 *J. Am. Chem. Soc.* **130** 12712
[19] P.Guimarães A 2009 *Principles of Nanomagnetism* (Berlin: Springer-Verlag)
[20] Hadjipanayis G C 1999 *J. Magn. Magn. Mater.* **200** 373
[21] Luborsky F E 1961 *J. Appl. Phys.* **32** S171
[22] Chen C H, Knutson S J, Shen Y, Wheeler R A, Horwath J C and Barnes P N 2011 *Appl. Phys. Lett.* **99** 012504
[23] Goll D, Berkowitz A E and Bertram H N 2004 *Phys. Rev. B* **18** 184432
[24] Yang C, Wu J J and Hou Y L 2011 *Chem. Commun.* **47** 5130
[25] Dormann J L, Fiorani D and Tronc E 1997 *Adv. Chem. Phys.* **98** 283
[26] Kneller E F and Hawig R 1991 *IEEE T. Magn.* **27** 3588
[27] Yang C and Hou Y L 2013 *Rare Metals* **32** 105
[28] Balamurugan B, Sellmyer D J, Hadjipanayis G C and Skomski R 2012 *Scripta Mater.* **67** 542
[29] Kim J, Barmak K, De Graef M, Lewis L H and Crew D C 2000 *J. Appl. Phys.* **87** 6140
[30] Jiang J S, Pearson J E, Liu Z Y, Kabius B, Trasobares S, Miller D J, Bader S D, Lee D R, Haskel D, Srajer G and Liu J P 2005 *J. Appl. Phys.* **97** 10K311
[31] Yang C, Jia L H, Wang S G, Gao C, Shi D W, Hou Y L and Gao S 2013 *Sci. Rep.* **3**
[32] Li W, Li X H, Li L L, Zhang J W and Zhang X Y 2006 *J. Appl. Phys.* **99**
[33] Liu F, Zhu J H, Yang W L, Dong Y H, Hou Y L, Zhang C Z, Yin H and Sun S H 2014 *Angew. Chem. Int. Edit.* **53** 2176
[34] Li W, Li L L, Nan Y, Li X H, Zhang X Y, Gunderov D V, Stolyarov V V and Popov A G 2007 *Appl. Phys. Lett.* **91** 062509
[35] Gabay A M, Zhang Y and Hadjipanayis G C 2004 *Appl. Phys. Lett.* **85** 446
[36] Cui W B, Takahashi Y K and Hono K 2013 *Adv. Mater.* **25** 1966
[37] Meiklejohn W H and Bean C P 1956 *Phys. Rev.* **102** 1413
[38] Nogues J and Schuller I K 1999 *J. Magn. Magn. Mater.* **192** 203
[39] Skumryev V, Stoyanov S, Zhang Y, Hadjipanayis G, Givord D and Nogues J 2003 *Nature* **423** 850
[40] Nogues J, Morellon L, Leighton C, Ibarra M R and Schuller I K 2000 *Phys. Rev. B* **61** R6455
[41] Zheng R K, Wen G H, Fung K K and Zhang X X 2004 *Phys. Rev. B* **69** 214431
[42] Stoner E C and Wohlfarth E P 1948 *Philos. Tr. R. Soc. S. A* **240** 599

[43] Apsel S E, Emmert J W, Deng J and Bloomfield L A 1996 *Phys. Rev. Lett.* **76** 1441
[44] Bucher J P, Douglass D C and Bloomfield L A 1991 *Phys. Rev. Lett.* **66** 3052
[45] Douglass D C, Cox A J, Bucher J P and Bloomfield L A 1993 *Phys. Rev. B* **47** 12874
[46] Zeng Y, Hao R, Xing B G, Hou Y L and Xu Z C 2010 *Chem. Commun.* **46** 3920
[47] Zhang W D, Xiao H M, Zhu L P and Fu S Y 2009 *J. Alloy Compd.* **477** 736
[48] Lu J, Jiao X L, Chen D R and Li W 2009 *J. Phys. Chem. C* **113** 4012
[49] Suber L, Imperatori P, Ausanio G, Fabbri F and Hofmeister H 2005 *J. Phys. Chem. B.* **109** 7103
[50] Hollinger R, Killinger A and Krey U 2003 *J. Magn. Magn. Mater.* **261** 178
[51] Choe S B, Acremann Y, Scholl A, Bauer A, Doran A, Stohr J and Padmore H A 2004 *Science* **304** 420
[52] Zhu J G, Zheng Y F and Prinz G A 2000 *J. Appl. Phys.* **87** 6668
[53] Chien C L, Zhu F Q and Zhu J G 2007 *Phys. Today* **60** 40
[54] Castano F J, Ross C A, Eilez A, Jung W and Frandsen C 2004 *Phys. Rev. B* **69**
[55] Jia C J, Sun L D, Luo F, Han X D, Heyderman L J, Yan Z G, Yan C H, Zheng K, Zhang Z, Takano M, Hayashi N, Eltschka M, Klaui M, Rudiger U, Kasama T, Cervera-Gontard L, Dunin-Borkowski R E, Tzvetkov G and Raabe J 2008 *J. Am. Chem. Soc.* **130** 16968
[56] Na H B, Song I C and Hyeon T 2009 *Adv. Mater.* **21** 2133
[57] Hao R, Xing R J, Xu Z C, Hou Y L, Gao S and Sun S H 2010 *Adv. Mater.* **22** 2729
[58] Henkelman R M, Stanisz G J and Graham S J 2001 *Nmr. Biomed.* **14** 57
[59] Zhao Z H, Zhou Z J, Bao J F, Wang Z Y, Hu J, Chi X Q, Ni K Y, Wang R F, Chen X Y, Chen Z and Gao J H 2013 *Nat. Commun.* **4** 2266
[60] Fortin J P, Wilhelm C, Servais J, Menager C, Bacri J C and Gazeau F 2007 *J. Am. Chem. Soc.* **129** 2628
[61] Rosensweig R E 2002 *J. Magn. Magn. Mater.* **252** 370
[62] Josephson L, Perez J M and Weissleder R 2001 *Angew. Chem. Int. Edit.* **40** 3204
[63] Perez J M, Josephson L, O'Loughlin T, Hogemann D and Weissleder R 2002 *Nat. Biotechnol.* **20** 816